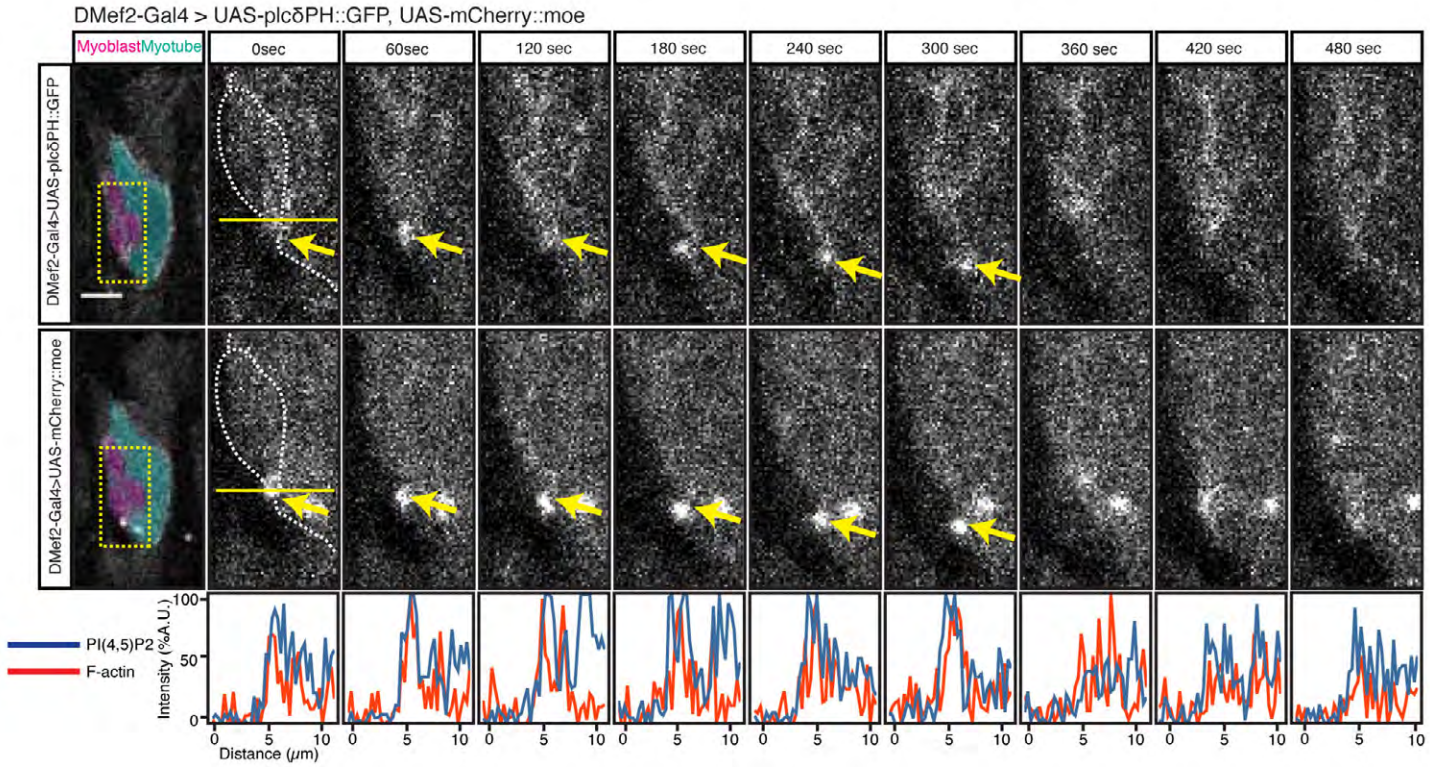

Supplementary Figure 1: PI(4,5)P2 enrichment at the fusion site as recorded through plcδPH::GFP reporter expression. Time lapse imaging of stage 14 embryos expressing UAS-plcδPH::GFP and UAS-mCherry::moe under the control of DMef2-Gal4, top and bottom panel, respectively. Clear enrichment of both signals are visible (arrows) and co-localize. Boxed area is magnified to highlight cell-cell interface. Strong enrichment of PI(4,5)P2 signal and moe::mCherry at the contact site is displayed in the overlapping peak in fluorescence intensity (yellow bar, line scan; a.u., lower panel). Frame rate 15sec, Scale Bar: 5 μm.

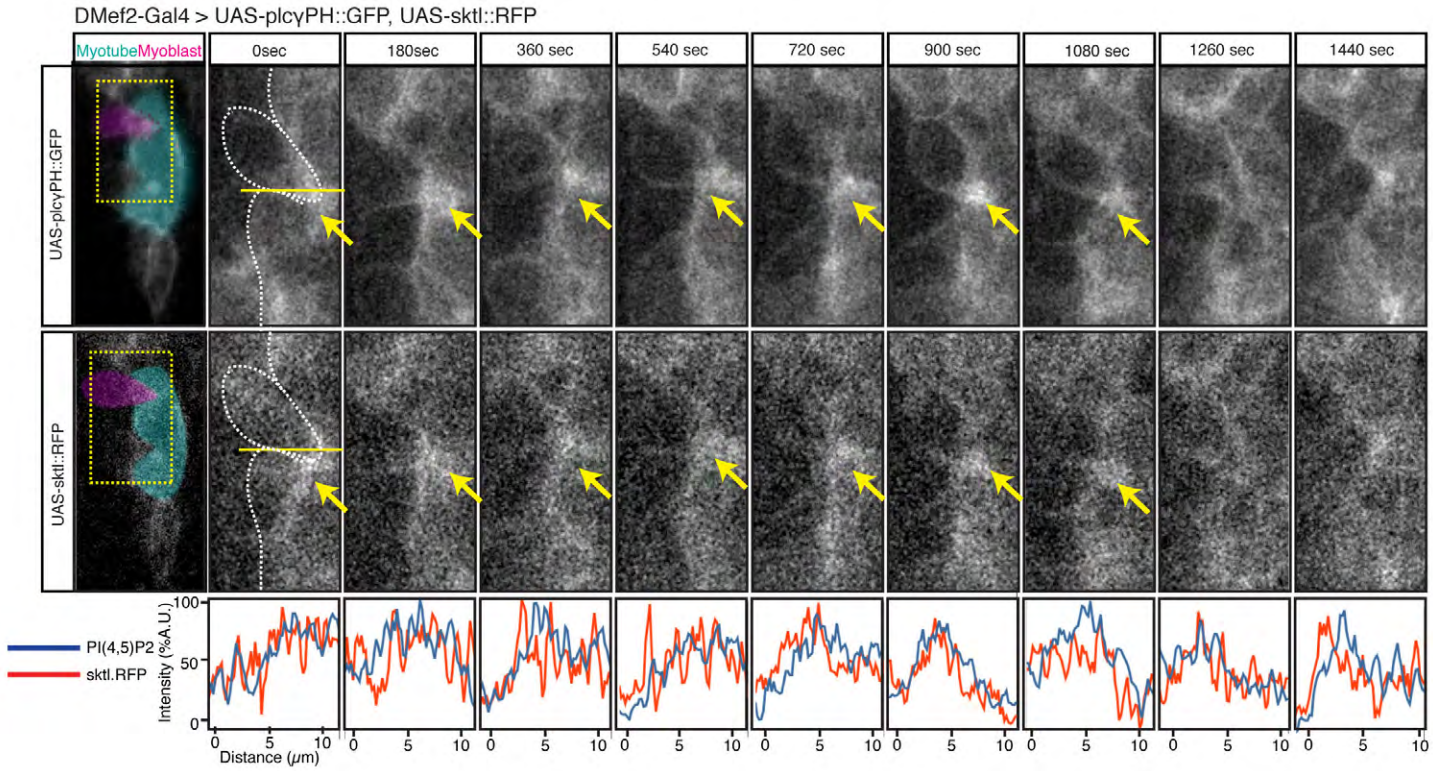

Supplementary Figure 2: Overexpression of sktI.WT::RFP does not affect fusion.

Time lapse imaging of stage 14 embryos expressing single copies of UAS-PH$^{plc\delta}$:GFP and UAS-sktI.WT:RFP under the control of DMef2-Gal4, top and bottom panel of A, respectively. Arrows indicate contact sites of FCMs (magenta) with the FC (turquoise). Signal for SktI.WT::RFP is enriched at the contact site, as is plcδPH::GFP. Fusion progresses normally with actual cell-cell fusion after 1440sec. Frame Rate 15 sec.

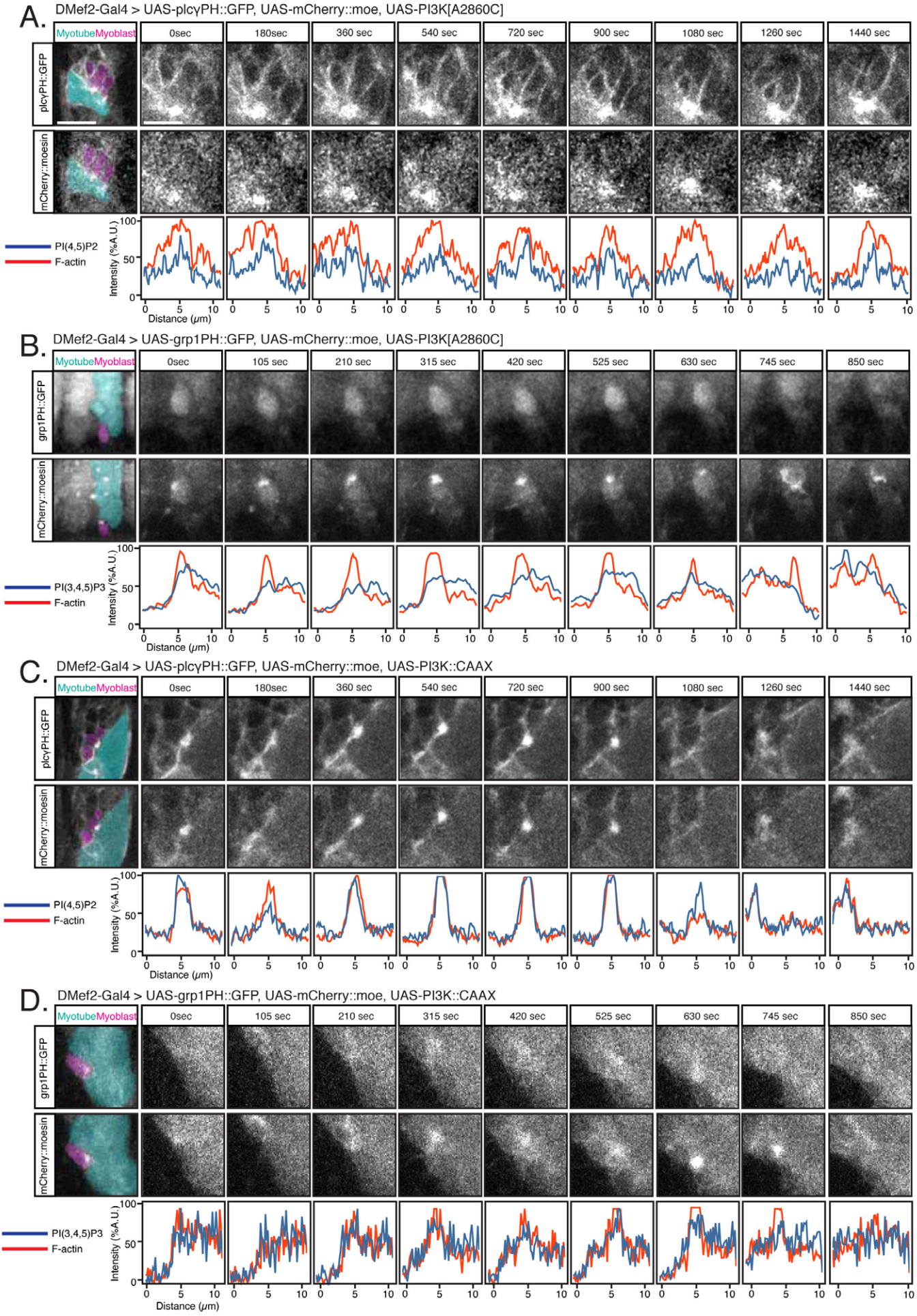
A.
DMef2-Gal4 > UAS-plcγPH::GFP, UAS-mCherry::moe, UAS-PI3K[A2860C]
MyotubeMyoblast
0sec
180sec
360 sec
540 sec
720 sec
900 sec
1080 sec
1260 sec
1440 sec
plcγPH::GFP
mCherry::moesin
PI(4,5)P2
F-actin
Intensity (%A.U.)
Distance (μm)
B.
DMef2-Gal4 > UAS-grp1PH::GFP, UAS-mCherry::moe, UAS-PI3K[A2860C]
MyotubeMyoblast
0sec
105 sec
210 sec
315 sec
420 sec
525 sec
630 sec
745 sec
850 sec
grp1PH::GFP
mCherry::moesin
PI(3,4,5)P3
F-actin
Intensity (%A.U.)
Distance (μm)
C.
DMef2-Gal4 > UAS-plcγPH::GFP, UAS-mCherry::moe, UAS-PI3K::CAAX
MyotubeMyoblast
0sec
180sec
360 sec
540 sec
720 sec
900 sec
1080 sec
1260 sec
1440 sec
plcγPH::GFP
mCherry::moesin
PI(4,5)P2
F-actin
Intensity (%A.U.)
Distance (μm)
D.
DMef2-Gal4 > UAS-grp1PH::GFP, UAS-mCherry::moe, UAS-PI3K::CAAX
MyotubeMyoblast
0sec
105 sec
210 sec
315 sec
420 sec
525 sec
630 sec
745 sec
850 sec
grp1PH::GFP
mCherry::moesin
PI(3,4,5)P3
F-actin
Intensity (%A.U.)
Distance (μm)

Supplementary Figure 3: Manipulation of PI(3,4,5)P3 levels do not generate myoblast fusion defects.

(A) Stills from time lapse imaging of stage 14 embryos expressing [UAS-PI3K(A2860C)], a PI3K92E dominant negative construct, with UAS-PH$^{plc\delta}$::GFP and UAS-mCherry::moesin. Fusion is affected, suggesting a sequestration effect of PI3k. DN together with PH$^{plc\delta}$::GFP (n=4). Expression of UAS-PI3K(A2860C) alone has no effect on fusion or myogenesis (data not shown). (B) Stills from time lapse imaging of stage 14 embryos expressing UAS-PI3K(A2860C) (PI3K92E dominant negative) with UAS-PH^{grp1}::GFP and UAS-mCherry::moesin. Fusion is not affected and PI(3,4,5)P3 remains cytoplasmic (compare to D, n=5). (C) Time lapse imaging of stage 14 embryos expressing UAS-PI3K.CAAX (PI3K92E constitutively active), with UAS-PH$^{plc\delta}$::GFP to detect PI(4,5)P2 and UAS-mCherry::moesin for F-actin. Accumulation of PI(4,5)P at the membrane and the cell contact sites indicate that neither PI(4,5)P2 nor fusion is affected (n=6). (D) Converse experiment to (B) using UAS-PI3K.CAAX with UAS-PH^{grp1}::GFP and UAS-mCherry::moesin. Fusion is not affected and PI(3,4,5)P3 accumulates slightly at the interface suggesting PI3k activity (compare to B, n=5). Frame rate 15sec. Scale Bar: 5 µm.

Supplementary Movie 1: PI(4,5)P2 accumulates at the adhesion site between FC/myotube and FCM.

Movie of time-lapse in Fig. 1A, single slice, lateral view of VA1 muscle (turquoise in first frame) with attached FCM (magenta in first frame) in a live DMef2-Gal4>UAS-PH$^{plc\delta}$::GFP embryo. Time lapse taken at stage 14 (11.5 h AEL), with the FCM firmly attached to the myotube. Over the acquisition time, PI(4,5)P2 becomes enriched at the cell-cell interface and disappears with the actual fusion event. Arrows point to accumulations of PI(4,5)P2; arrowheads to filopodia. Red arrow indicates fusion event with the disappearance of the FCM, purple arrow points to opening in the fusion interface just before fusion. Frame rate 45 sec, scale bar: 5 µm

Supplementary Movie 2: PI(4,5)P2 colocalizes with the F-actin focus.

Movie of time-lapse in Fig. 1B, single slice, lateral view of VA1 muscle (turquoise in first frame) with attached FCM (magenta in first frame) in a live DMef2-Gal4>UAS-PH$^{plc\delta}$::GFP, UAS-mCherry::moe embryo. Time lapse taken at stage 14 (11.5 h AEL), with the FCM firmly attached to the myotube. Over the acquisition time, the PI(4,5)P2 enrichment overlaps temporally and spatially with F-actin at the cell-cell interface and disappears with the actual fusion event. Arrows point to accumulations of PI(4,5)P2; arrowheads to filopodia. Red arrow indicates fusion event with the disappearance of the FCM. Frame rate 45 sec, scale bar: 5 µm.

Supplementary Movie 3: PI(3,4,5)P3 does not colocalize with the F-actin focus.
Movie of time-lapse in Fig. 1C, lateral view of VA1 muscle (turquoise in first frame) with attached FCM (magenta in first frame) in a live DMef2-Gal4>UAS-PH^{grp1}::GFP, UAS-mCherry::moe embryo. Time lapse taken at stage 14 (11.5 h AEL), with the FCM firmly attached to the myotube. Over the acquisition time, no PI(3,4,5)P3 enrichment was detected nor did PI(3,4,5)P3 colocalize with the F-actin focus at the cell-cell interface. Frame rate 15 sec, scale bar: 10 µm.

Supplementary Movie 4: PI(4,5)P2 accumulates at the fusion site in the membrane of the FC/myotube.
Movie of time-lapse in Fig. 2A, lateral view of VL1 muscle with attached FCM in a live 5053-Gal4>UAS-PH$^{plc\delta}$::GFP embryo. Time lapse taken at stage 14 (11.5 h AEL), with the FCM firmly attached to the myotube. Over the acquisition time, PI(4,5)P2 becomes enriched at prospective cell-cell interfaces, upon cytoplasmic mixing the FCM can be detected by the GFP signal. Frame rate 60 sec, scale bar: 10 µm.

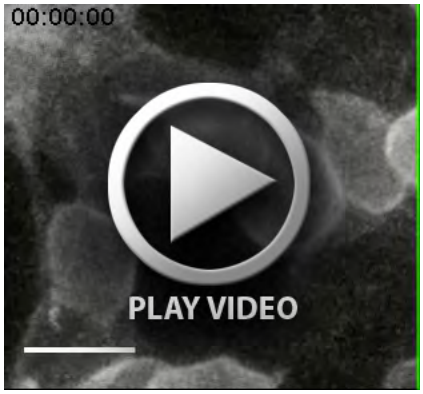

Supplementary Movie 5: PI(4,5)P2 is enriched at the fusion site in the FCM.
Movie of time-lapse in Fig. 2B, lateral view a live sns-Gal4>UAS-PH$^{plc\delta}$::GFP mbc[c1] homozygous embryo. Time lapse taken at stage 14 (11.5 h AEL), with the FCMs attached to FCs. Over the acquisition time, PI(4,5)P2 stays enriched at the cell-cell interface and does not dissolve due to the fusion defect. Frame rate 45 sec, scale bar: 5 µm.

Supplementary Movie 6: Expression of a kinase dead version of Sktl blocks fusion.
Movie of time-lapse in Fig. 4B, unidentified myotube with attached FCMs in a live 2xDMef2-Gal4>2xUAS-sktl.KD::RFP embryo. Time lapse taken at stage 14 (11.5 h AEL), with the FCMs firmly attached to the myotube. Over the acquisition time, no fusion event resolves. Note that Sktl.KD::RFP is enriched at the cell-cell contact sites. Frame rate 15 sec, scale bar: 5 µm.

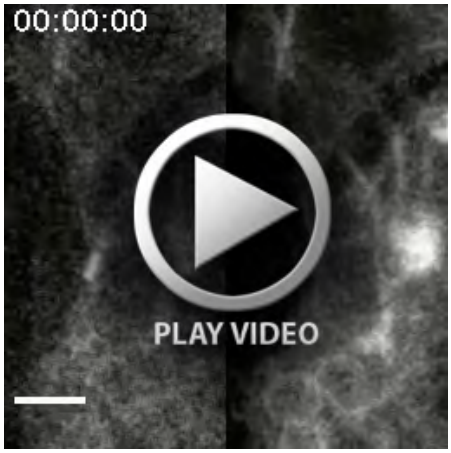

Supplementary Movie 7: Expression of kinase dead Sktl with plcδPH::GFP blocks fusion.
Movie of time-lapse in Fig. 4C, unidentified myotube with attached FCMs in a live DMef2-Gal4>UAS-sktl.KD::RFP, UAS-$PH^{plc\delta}$::GFP embryo. Time lapse taken at stage 14 (11.5 h AEL), with the FCMs firmly attached to the myotube. Over the acquisition time, no fusion event resolves. Note that Sktl.KD::RFP (left hand frames) and $PH^{plc\delta}$::GFP (right hand frames) is enriched at the cell-cell contact sites. Frame rate 15 sec, scale bar: 5 µm.

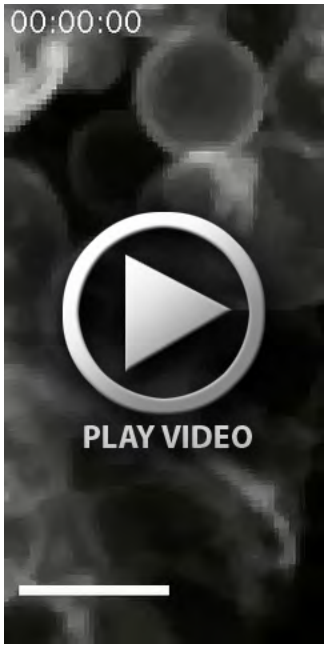

Supplementary Movie 8: FCM behavior under conditions of PI(4,5)P2 sequestration.
Movie of time-lapse in Fig. 5D, unidentified myotube with attached FCMs in a live 2x DMef2-Gal4> 2xUAS-PH$^{plc\delta}$:GFP embryo. Time lapse taken at stage 14 (11.5 h AEL), with the FCMs firmly attached to the myotube. Over the acquisition time, no fusion event resolves. Note that the FCM is attached to the myotube/FC through a single extension but unable to align its cell body with that of the fusion partner. Frame rate 30 sec, scale bar: 5 µm.

Supplementary Table S1: Approaches used to disrupt PIP pathway enzymes

The following genotypes were examined for defects in fusion, attachment or morphology: none was found under standard laboratory conditions.

Genotype
sktl[5]
sktl[15]
sktl[20]
sktl[20]/sktl[5]
sktl[20]/sktl[15]
fwd[Neo]
fwd[EY05397]
fwd[B347]
sktl[20]/fwd[Neo]
sktl[20]/fwd[EY05397]
sktl[20]/fwd[B347]
twi-Gal4>UAS-sktl.RNAi KK
twi-Gal4>UAS-sktl.RNAi TRiP
Dmef-Gal4>UAS-sktl.RNAi KK
DMef2-Gal4>UAS-sktl.RNAi TRiP
twi-Gal4; DMef2-Gal4> UAS-sktl.RNAi KK
twi-Gal4, DMef2-Gal4>UAS-sktl.RNAi TRiP
UAS-Dcr2; Twi-Gal4>UAS-sktl.RNAi KK
UAS-Dcr2; Twi-Gal4>UAS-sktl.RNAi TRiP
UAS-Dcr2;; DMef2-Gal4>UAS-sktl.RNAi.KK
UAS-Dcr2;; DMef2-Gal4>UAS-sktl.RNAi.TRiP
otu-Gal4; nos-Gal4>UAS-sktl.RNAi TRiP X DMef2-Gal4>UAS-sktl.RNAi TRiP
sktl[Δ20]; DMef2-Gal4> sktl[20]; UAS-sktl.RNAi TRiP

Supplementary Table S2. Stocks used

Mutants	References
blow$^{[1]}$	Doberstein et al., 1997
rols$^{[T627]}$	Chen and Olson, 2001
Df(1)w67k30 [deficiency removing *duf* and *rst]*	Ruiz-Gómez et al., 2000
sns$^{[XB3]}$	Bour et al., 2000
sing$^{[27]}$	Estrada et al., 2007
mbc$^{[c1]}$	Rushton et al., 1995
kette$^{[J4-48]}$	Hummel et al., 2000
loner$^{[T1032]}$	Chen et al., 2003
Dwip$^{[D30]}$	Massarwa et al., 2007
sltr$^{[S1946]}$	Kim et al., 2007
wsp$^{[3D3-035]}$	Schäfer et al., 2007
scar$^{[Δ37]}$	Zallen et al., 2002
Rac1$^{[J11]}$,*Rac2*$^{[Δ]}$, *Mtl*$^{[Δ]}$	Hakeda-Suzuki et al., 2002
sktl^{Δ5},	Hassan et al., 1998
sktl^{Δ15},	Hassan et al., 1998
sktl^{Δ20},	Hassan et al., 1998
fwd$^{[B347]}$	Bloomington 16204
fwd$^{[EY05397]}$	Bloomington 16654
fwd$^{[Neo1]}$	Brill et al., 2000
GAL4 lines	
DMef2-GAL4	Ranganayakulu et al., 1998
5053-GAL4	Ritzenthaler et al., 2000
rP298-GAL4	Dutta et al., 2002
twist-GAL4	Baylies and Bate, 1996
UAS lines	
UAS-mCherry::moe^{act}	Vilmos et al., 2009
UAS-PH^{plcγ}*::GFP*	Pinal et al., 2006
UAS-PH^{plcδ}*::GFP*	Verstreken et al., 2009
UAS-sktl.WT::RFP	Raghu et al., 2009
UAS-sktl.KD::RFP	Raghu et al., 2009
UAS-PH^{grp1}*::GFP*	Pickering et al., 2013
UAS-norpA	Kwon et al., 2008
UAS-EGFP::HA::synaptojanin	Dickman et al., 2006
UAS-insp54	Varnai et al., 2006; this study
UAS-PI3K92E.CAAX	Bloomington 8294
UAS-PI3K92E.A2860C	Bloomington 8289
UAS-sktl.RNAi (KK105246)	VDRC v101624
UAS-sktl.RNAi (TRiP.GL00072)	Bloomington 35198
UAS-sktl.RNAi (TRiP.JF02796)	Bloomington 27715
Other transgenes	
ap^{ME}*-NLS::dsRED*	Richardson et al., 2007